Real-time Diagnostics of Gas/Water Assisted Injection Moulding using Integrated Ultrasonic Sensors

L. Mulvaney-Johnson[1], C. C. Cheng[2], Y. Ono[3], E. C. Brown[1], C. K. Jen[2], P. D. Coates[1]

1) IRC in Polymer Science and Technology, University of Bradford, BD7 1DP, UK

2) Industrial Materials Institute, National Research Council Canada, Boucherville, Quebec, Canada.

3) Dept. of Electrical and Computer Engineering, McGill University, Montreal, Quebec, Canada.

.

Footnote to be made on authors:

C C Cheng's permanent address is now: Dept. of Electrical Engineering, Hsiuping Institute of Technology, Da-Li, Taichung, Taiwan.

Y. Ono's permanent address is now: Dept. of Systems and Computer Engineering, Carleton University, Ottowa, Ontario, Canada.

Abstract

An ultrasound sensor system has been applied to the mould of both the water and gas assisted injection moulding processes. The mould has a cavity wall mounted pressure sensor and instrumentation to monitor the injection moulding machine. Two ultrasound sensors are used to monitor the arrival of the fluid (gas or water) bubble tip through the detection of reflected ultrasound energy from the fluid polymer boundary and the fluid bubble tip velocity through the polymer melt is estimated. The polymer contact with the cavity wall is observed through the reflected ultrasound energy from that boundary. A theoretically based estimation of the residual wall thickness is made using the ultrasound reflection from the fluid (gas or water) polymer boundary whilst the samples are still inside the mould and a good correlation with a physical measurement is observed.

1. Introduction

The area of fluid assisted polymer processing covers both single and two phase fluid / polymer combinations, this work is concerned with the two phase gas and water assisted injection moulding processes. The two phase implementation of fluid assisted moulding typically utilises either gas or water as the fluid and there is a distinct boundary between the fluid and the polymer melt; a single bubble is intended to form leaving the article hollow. The advantages of both gas and water assisted moulding are very similar and both can be utilised to manufacture thick sectioned items by gas or water penetration through the melt to "core-out" the article. Gas assisted moulding has been in existence for many years and has been utilised to manufacture items such as suitcase handles, grab handles and core out rib junctions. More recently water assisted moulding has developed to increase the heat transfer from the moulten polymer to the fluid which has the effect of reducing product cycle time. In addition, the water process has typically seen smoother surface finish of the residual wall inner surface and an overall thinner wall when compared to gas assisted processing. The foaming of the inner wall often observed with gas assist is thought to be caused by the dissolution of the gas into the melt that later precipitates to form local surface foam. The improved surface finish from the water process offers the potential to form media ducts with smooth internal bores where the risk of particulate break off has been minimised and viscous drag reduced. The main advantages of the water and gas assisted moulding processes over the conventional process include the ability to provide an even and reduced pressure distribution within the mould during cooling, which can reduce post moulding warpage for reasons previously outlined; improvements in "sink" where the expansion of the pressurised fluid bubble compensates for contraction of the polymer during cooling and therefore maintains polymer contact with the cavity walls; material savings can be realised in the "short-shot" process configuration[1,2].

A further variation of the gas assisted moulding process is the application of gas between the mould wall and polymer melt. This configuration usually requires the mould to be gas sealed to contain the gas pressure within the mould. The gas is applied to the non-aesthetic surface of the product and is particularly beneficial for reducing warpage in flat mouldings designed with strengthening ribs to provide a well formed "A" surface that is "pushed" against the cavity during cooling[3].

The work presented here focuses upon the two phase water and gas assisted injection moulding processes. The injection moulding machine and the mould tool are fitted with instrumentation, including ultrasound, to monitor the progress of the melt and water / gas as it penetrates through the melt in a fixed section of the cavity. The test

specimen is a long flow path tube with an initial Ø20mm and then Ø10mm section that is "cored out" using the gas or water assist. The test specimen is representative of the thick section tubular components that the gas assist process has been used to manufacture. The applications for water assisted components have been noted in the literature to be automotive media ducts, door handles and thick sectioned components of a child's tricycle[4].

A further variation of fluid assisted processing is the single phase homogeneous system that relies upon the dissolution of a fluid such as CO_2 or N_2 into the polymer melt followed by significant mixing to provide a homogeneous melt. The resultant melt typically exhibits a reduction in viscosity compared with no addition of fluid, which is beneficial for applications that would benefit from lower pressures during processing. The dissolved fluid has a tendency to precipitate from solution with a lowering of local temperature and pressure to form small bubbles within the melt. The foaming from these small bubbles can be problematic for extruded profiles, where profile accuracy is a quality requirement. However, the foaming action can be useful within an injection moulded product where completion of mould filling at relatively low pressure is beneficial to reduce post moulding warpage through the reduction of frozen residual stress normally introduced through high injection and "packing" pressures. Due to the formation of bubbles at the melt front the surface finish of the product is typically rough and this process is aimed at structural non-aesthetic products. However, the introduction of pre-pressurised moulds[5] to maintain the gas in solution at the melt front during filling has aimed to improve the surface finish significantly.

2. Method of mould based ultrasonic diagnostics and sensors

Ultrasonic signatures such as propagation characteristics (velocity and attenuation), reflection and transmission coefficients, and scattering signals from materials, are associated with physical and rheological properties of materials (phase, viscosity, microstructure, chemical composition, density, molecular weight, filler concentration, etc.), process dynamics (cycle, injection, packing, holding, cooling, mould open, ejection, etc.), material dynamics (melting, flow arrival and advancement, filling completeness, solidification, shrinkage, detachment, etc.), process parameters (temperature, pressure, etc.) and product qualities (uniformity, shape, surface flatness, deformation, inclusions, voids, etc.). Thus, these signatures can be used for diagnostics of polymer processes and product quality[6-13]. For such purposes, ultrasonic transducers (UTs) are attached onto the extrusion barrel and/or mould (mould insert) of injection moulding machines.

Figure 1 shows a cross-sectional schematic view of a conventional injection moulding tool fitted with the UTs and data acquisition system using an ultrasonic pulse-echo technique. Ultrasonic waves radiated from the UTs propagate through both the mould insert and polymer, reflections at the material interfaces within the propagation paths are received by the same UTs. Echoes L^n (where n=1,2,3, etc) are the n^{th} round trip longitudinal echo reflected at the nearest cavity wall interface. This interface is either steel/air or steel/polymer, depending on if polymer has arrived at that location.. Echos L_n (where n=1, 2, 3, etc) are the nth round trip longitudinal echo from the furthest polymer/steel interface. Both the time delay and amplitude variations of these echoes are used to measure the ultrasonic velocity and signal attenuation through the steel and polymer materials. The steel conditions are relatively constant and the propagation of the ultrasound signal within the polymer is related to local pressure and temperature which in turn reflects the process conditions. A Multiple sensor configuration enables monitoring of the melt flow in the mould cavity and polymer status at the chosen locations. The ultrasonic data acquisition system was composed of two pulser-receivers (Panametrics Inc., Waltham, MA), an 12-bit dual-channel digitizing boards (Gage Applied Science Inc., Montreal, QC, Canada) with a sampling rate of 50MHz for each channel and a personal computer with a data acquisition and analysis program by LabVIEW. The acquisition rate was 100Hz.

The developed high temperature ultrasonic transducer (HTUT) has overcome some of the key practical issues for application to industrial polymer processes at elevated temperatures[14,15]. Limitation include been the degradation of couplant between the transducer and the steel surface along with the need for a cooling system for the transducer, that add complexity to the application and could induce thermal changes to the process. Three piezoelectric HTUT sensors were directly integrated onto a mould insert of a gas/water-assisted injection moulding machine (TM1300 from Battenfeld). The polymer side of the mould insert had a half cylindrical cavity with a radius of 10mm and three UTs (UT-A, B, C) were fabricated at the HTUT side with an interval of 35mm, as shown in Figures 2a and 2b, respectively. Figure 2c presents a moulded part with an inset of a cross-section of the part at the UT-A area, where three black dots indicate the corresponding areas of the UTs. These UTs had a centre frequency of 9 MHz and 6dB bandwidth of 6 MHz. Fig. 3a and 3b presented the performances of UT-A. L^n (n =1, 2) represents n^{th} round trip longitudinal echoes propagating in the HTUT sensor insert and reflecting within the mould insert/air interface. Signal-to-noise ratio (SNR) of the first round trip longitudinal wave echo, reflected at the substrate/air interface measured in pulse-echo technique, was above 30dB at room temperature. In addition, it was confirmed that these sensors could be operated up to 200°C. Such performance is sufficient for monitoring of polymer

water/gas injection molding processes where the mould insert bulk temperature is likely to peak at around 100°C when processing certain polymeric materials.

Figure 4 presents a schematic cross-section of the gas and water assisted mould with the UTs, showing ultrasonic propagation paths and flows of polymer melt and fluid (gas or water) within the cavity during the moulding cycle. L_S is the longitudinal echo that is reflected from the interface between the "frozen layer" of polymer near the mould wall and the remaining polymer melt. $L_{G(W)}$ is the longitudinal echo reflected at the liquid/gas (water) interfaces. In Figure 4, ultrasound partially transmits to water during water-assisted injection moulding, resulting in less reflected ultrasonic energy when compared with gas-assisted moulding; this will be further discussed later.

A cavity sensor with combined pressure and temperature sensing capabilities (Kistler type 6190A) was flush mounted to the mould cavity in a location opposite the UT-B transducer. This arrangement allowed for the polymer temperature and pressure at the mould wall to be measured for comparison with the ultrasonic data; figure 4 shows schematically the positioning of the transducers.

3. Experimental setup

The gas and water assisted injection moulding processes were operated on an injection moulding machine at the University of Bradford, UK. The injection mouding machine, shown in figure 5, was a Battenfeld TM1300 / 350 + 210 BM fitted with a B4 controller. This machine has the capability to deliver two different polymer melts to the mould (skin and core materials), but in this case only one of the available injection barrels was utilized as only a single material was required. The Barrel A is ∅40mm internal diameter with a maximum specific melt pressure of 160MPa and maximum melt delivery rate of 132ccm/s.

A specially designed mould tool was utilized for preparation of the gas and water assisted samples, a photograph of the actual tool mounted on the machine platens is shown in figure 6. The tool is comprised of a main cavity plate that houses inserts containing the mould cavity form and exchange of the cavity inserts allows for different forms and flow lengths to be studied; the cavity form was not changed for the work presented here. The polymer melt is injected into the cavity at the location shown and follows a runner to the bottom of the tool where the fluid injection needle is located. The needle is located at the bottom of the tool, which is a requirement for successful extraction of the water using gravity at the end of the moulding cycle. Shown in figure 6 is the insert containing the instrumented straight ∅20mm tubular region of the sample. This section is instrumented with pressure, temperature and ultrasound transducers that coincide in position along the section to provide data from

the same locations. The combined pressure and temperature transducer (close up of ∅4mm sensor shown in figure 6) is positioned at the same location along the tube specimen and opposite to the ultrasound transducer "B"; ultrasound transducers and their locations are discussed later.

The "short shot" method was used to manufacture these specimens, where the mould cavity is partially filled with polymer (the short shot) prior to the injection of either gas or water. The fluid bubble displaces the polymer melt to the end of the cavity in order to complete filling and the final specimen becomes hollow with either a gas or water core, depending upon the process. Prior to the mould opening the high pressure gas or water is released from the mould to leave a hollow article.

The material used here was high density polyethylene (HDPE) from BP chemicals (BP Rigidex HD5050EA), which has good ultrasound propagation properties. Single melt and mould temperature settings of 250°C and 30°C respectively where used throughout and these are the mid point settings suggested by the material manufacturer. The melt injection rate was set to be 60ccm/s over the entire 135ccm melt delivery phase. However, since the peak available injection pressure was reached during the melt injection phase, the actual injection rate was measured to be around 40ccm/s. The fluid injection pressures where changed in these experiments in order to change the residual wall thickness and therefore bubble front velocity[16-18] if the bubble propagation could be interpreted from the ultrasound data and if changes to the residual wall thickness could be monitored. The gas and water injection pressure settings were 10, 12, 20MPa, and 17.5, 20, 25MPa, respectively. The fluid pressure was increased to the set value in a single step, held for 6.0s and then the system valves where closed for a further 10s before the fluid pressure was released.

4. Results

The experimental results for the gas assisted injection moulding experiments are presented, where specimens were moulded with gas injection pressures of 10, 12 or 20MPa. Figure 7 shows a typical result of acquired ultrasonic signals from UT-A during one cycle of gas assisted injection moulding using the ultrasonic pulse echo technique. The L^1 and L^2 echoes are clearly marked on the data and correspond to the 1st and 2nd round trip echoes between the transducer and cavity surface. The L_S and L_G echoes are also clear and correspond to the echo from the frozen layer/polymer melt interface and the polymer melt/ gas interface respectively. At around a process time of 9.2s the L_G echo starts to appear, indicating that the gas bubble front was first observed at the UT-A location at this time. Both the L_G and L_S echo remains evident up to a process time of 27s, at which point the gas pressure is released and the polymer may detach from the cavity wall. Detachment from the cavity wall is

driven by the shrinkage of the polymer during cooling and associated phase change. The changing time delay of the L_S and L_G echoes may be evidence that the polymer was still in the melt phase during this time. In the process time from 9s to 27s, the time delay of the L_G echo varied from 14.5μs to 13μs indicating that the solidification, temperature reduction of the part and the wall thickness reduction due to the movement of gas bubble. However, in the same period, the variation of the L_S echoes only implied the solidification and temperature reduction of the part. It is noted that the small echoes S^n (n=1, 2) always appearing at the time delay of 9μs and 12μs are the shear-wave signals propagating in the mold insert.

Results from a typical water assisted moulding cycle are presented in figure 8 where the water injection pressure is 20MPa. This figure shows the ultrasonic signal data from UT-A with the familiar L^1, L^2 and L_S echoes indicated. The L_W echo appears around the process time of 10s with the time delay of around 12.5μs is an echo reflected from the polymer/water interface. This L_w echo is difficult to detect as the signal-to-noise ratio is low, certainly when compared with the L_G echo (gas assist) in figure 7. The reason for the difference is a much lower ultrasound reflection coefficient at the polymer/water interface of 0.2 compared with a reflection coefficient of around 1.0 for the polymer/gas interface. In effect, these coefficients indicated that 20% of ultrasound was reflected at the polymer/water interface in water assisted injection moulding while around 100% (total reflection) of the signal is reflected at the polymer/gas interface[15]. In addition, voids within the wall of water moulded samples where observed that scattered and/or attenuated the ultrasonic signals propagating within the wall. Due to the weak reflected signal from the bubble interface in water assisted moulding no further comparison work was possible with this body of data.

In order to investigate further the correlation between the ultrasonic signals observed and the gas assisted moulding cycle a process time based comparison is made between the amplitude values of the L^2 and L_G echoes (Figure 7) and the gas pressure control signal and cavity wall pressure at the UT-B location. Results showing the L^2 and L_G echos with respect to process time are presented in figure 9. The gas pressure control signal and cavity wall pressure with respect to process time are shown in figure 10. The L^2 echo was chosen instead of the L^1 echo since, in principle, higher-order round trip echoes of L^n can lead to a higher sensitivity to the cavity wall interface condition[19]. In figure 9, at process time of 6.3s, the polymer melt arrived at the cavity area beneath the UT-A, since the amplitude of the L^2 echo decreased as an increasing proportion of the ultrasonic energy was transmitted into the polymer through the cavity wall/polymer interface. Figure 10 shows that around this time the cavity pressure started to increase, indicating arrival of the polymer melt at the UT-B

location. Thus average polymer melt speed, V_m, during this melt injection phase can be estimated from the time difference (Δt_m) between the fall in L^2 echo amplitude at UT-A and the increase of the cavity pressure at the UT-B location by equation 1:

$$V_m = L/\Delta t_m \qquad (1)$$

where L=35mm and is the distance between the UT-A and UT-B locations. The average polymer melt speed is around 175mm/s, however other process signals contradict this value of melt front velocity, which is discussed later.

At 8.3s (figure 10) the gas injection control signal begins to rise, which should correspond to the injection of gas at the gas needle. The amplitude of the L_G echo increases significantly at 9.2s (figure 9), which indicates that the gas bubble interface with the melt has suddenly appeared at the UT-A location. The L_G echo amplitude stays high, but the L_G signal becomes indeterminate when its transit time coincides with that of the L^2 echo due to signal superposition between 13.8s and 21.7s of process time. The amplitude of the L^2 and L_G echoes have been blanked out during this time interval in figure 9 and this particular phenomenon can be seen more clearly in figure 7.

In figure 10, from 6.5 to around 8.0s, the steady rise in cavity wall pressure is due to the melt pre-filling phase. Once melt pre-filling is complete the cavity wall pressure falls rapidly until gas injection takes place at 8.3s (the associated gas injection control signal rises at this time). From 8.3s to around 10.5s The cavity pressure rises during gas bubble penetration and the equalising of pressure across the needle (between the line supply and the gas bubble). The set gas pressure is maintained for 6.0s and then from a process time of 14.0s to 24s the gas valves are closed during a period termed “vent delay time”. The cavity pressure during this vent delay time gradually falls as both the gas bubble volume increases due to melt shrinkage and escape of gas from the system (probably through the needle/polymer seal that forms). At 27.5s, the amplitudes of both the L^2 and L_G echoes recovered to their initial values as the gas pressure was released from the system. This infers that the polymer has detached from the cavity wall since the condition at the cavity wall for ultrasound is the same as t=0s, i.e. no melt present. The detachment of the specimen from the mould wall is not unexpected as shrinkage of the polymer during cooling is known to take place. The process time from 6.3s, the amplitude of the L^2 echo decreased, to 27.5s, the amplitude of the L^2 echo recovered to the initial value, was called ultrasonic contact duration. The contact duration may indicate the period during which the specimen and mould are in contact and helps to evaluate the cooling efficiency. This information will be discussed further in section 5-4.

5. Discussion

5-1 Melt pre-filling

Melt pre-filling, or short shot, provides a known quantity of polymer melt to the cavity prior to the injection of either gas or water. Since the movement of the melt injection piston, or screw, has been recorded during this melt injection phase an estimate of the melt injection rate can be made. Assuming incompressibility of the polymer melt and no back flow of polymer over the piston during its forward movement, then the rate of piston volumetric displacement is equal to the volumetric flow rate within the ∅20mm section of the mould cavity, where the UTA, UTB and pressure transducers are located. Figure 11 shows two process signals, which are melt volume in front of the melt injection piston and cavity wall pressure at location UTB taken from the Kistler piezoelectric pressure transducer. The third signal plotted on figure 11 is rate of change of melt volume in front of the injection piston, which is differentiated from the volume signal already plotted. The rise in cavity wall pressure at UTB is noted in figure 11 and corresponds to an increase in melt pressure at that point. If the melt was flowing in the usual fountain flow regime this pressure rise would indicate the arrival of the melt flow front, as shown schematically within this figure. The melt volume between the UTA and UTB locations is 11ccm and the time taken for the injection piston to deliver this is 0.5s, therefore the average volumetric flow rate is 22ccm/s. The corresponding average melt flow front velocity between UTA and UTB, which are 35mm apart, is therefore 70mm/s. It is worth noting at this point that the set volumetric flow rate of the piston was 60ccm/s, but due to the required injection pressure being above 80% of that available from the machine (160MPa) the actual injection rate was lower.

Examination of the UTA and UTB signal amplitude data reveals that the actual melt front velocity is apparently much higher than that calculated from the movement of the melt injection piston. Figure 12 shows a fall in the amplitude of the L^2 echo upon arrival of the polymer melt at each of the UTA and UTB transducer sites. The second plot shows the corresponding cavity wall pressure rise at the UTB site. The time difference between these apparent melt arrival events is around 0.15sec, which would give a corresponding melt flow rate of 73ccm/s and melt front velocity of 233mm/s. The melt flow rate determined from this data is higher than even the machine set point of 60ccm/s.

The photograph of part of the melt pre-filling pattern is shown in figure 13 and provides a clue as to this discrepancy between the theoretical and apparent melt front velocity. The pre-filled sample shown is part of the full pre-fill in order to show the approximate the melt distribution in the region of the UT's and pressure sensor. The sample has clearly been formed by a coiled tube of molten polymer melt extruded

from the ∅4mm gate into the much larger ∅20mm section. This phenomenon is often termed “jetting” since a jet of polymer melt is project into the cavity rather than a smooth fountain flow. The jet of melt is likely to have come into contact with the mould wall in the UTA and UTB locations, therefore reducing the echo amplitude as ultrasound energy passes directly into the localised polymer. This phenomenon is thought to be responsible for the apparently premature arrival of the melt at the UTB location when compared the known volumetric flow rate into the mould.

5-2 Gas flow speed

Tracking the flow front speed of the gas bubble over moulding cycles may present an opportunity to detect needle blockages or reductions in gas supply pressure to the mould. Figure 14 presents the amplitude variations of the L_G echoes, measured by UT-A and UT-B, with respect to the process time. The L_G echoes began to be observed at 9.2s and 9.7s with the UT-A and UT-B, respectively, when gas arrived at each UT location. Therefore, gas flow speed (V_f) could be estimated using the time differences (Δt_f) of appearances of the L_G echoes at the UT-A and UT-B locations by: $V_f = L/\Delta t_f$, where L (=35mm) is the distance between the UT-A and UT-B. The results are presented in Figure 15. Gas flow speed increased with gas pressure. The bubble speed is linked to the formation of the RWT, where higher speed (higher pressure) results in a thinner RWT. In addition, these data provide valuable insights into the actual processing conditions that can be utilized to validate the results from mould filling simulations.

5-3 Wall thickness

Quality control to evaluate the wall thickness of the moulded part is crucial for fluid assisted injection molding. But currently the measuring method was limited to off-line techniques, in which the parts are cut to measure the wall thickness. Thus, real-time ultrasonic thickness measurement of the parts was conducted during fluid assisted injection molding process. After moulding, the moulded parts were sectioned and a thickness gauge, with the accuracy of ±1μm, was used to measure wall thickness at the locations corresponding to the UT-A and UT-B positions in Figure 2. The measuring results of wall thickness for gas/water assisted injection molding are shown in Figure 16 and 17, respectively. In these two figures, the closed squares (■) and circles (●) represented the measured wall thickness by a thickness gauge at the UT-A and UT-B areas, respectively. The wall thicknesses at the UT-B (●) were greater than those at the UT-A (■) close to the gas/water injection nozzle, except for part #9 in Figure 16 and part #2 in Figure 17. This anomaly is thought to be an end effect since the UT-A location is close to the tapered transition section where gas flow

rate is expected to be unsteady or the unsteady water flow when the water pressure was low.

The wall thicknesses were estimated by equation 2

$$h_m = \frac{1}{2} V \Delta t_m \qquad (2)$$

m = G, W

where h_m is wall thickness estimation in mm, V is ultrasonic velocity in the polymer, and Δt_G and Δt_W are the time delay difference between L^1- L_G and L^1 - L_W in Figure 7 and 8, respectively. The time delay differences of Δt_G and Δt_W were chosen at the process time of 27.0s in Figure 7 and 11.0s in figure 8, respectively. These timings were just before the L_G and L_W echoes disappeared. In the estimation, the ultrasonic velocities of 1108m/s and 1297m/s in the polymer just before the part detachment were used to calculate the wall thicknesses for gas/water assisted injection molding, respectively. These velocities were obtained using the time delay differences and the measured wall thicknesses at 20MPa. The estimations of wall thickness using the ultrasound data are given in Figures 16 and 17 with open squares (□) and circles (○) to denote UT-A and UT-B, respectively. It is noted that, in Figure 17, parts #1, 4 and 5 cannot provide estimated wall thicknesses at UT-B, and part #5 cannot provide that at UT-A. In Figure 16, the measured and estimated wall thicknesses had good agreement within an accuracy of ±7% except for the parts #5 at the UT-B and #9 at the UT-A, indicated by the arrows. In Figure 17, the agreement was within an accuracy of ±10% except for the parts #2 at the UT-B, indicated by the arrow. This suggests that water bubble inclusions within the residual wall may have provided an early echo that appeared to be a thinner than actual residual wall.

5-4 External Diameter distribution

Fluid assisted injection molding incorporated gas or water injection in the mold filling cycle to form the hollow components. Therefore, to keep the hollow structure from deformation is the basic requirement for part quality. In our experiments, the gas/water was injected into the mold during the filling process with the pressure of 10, 12, 20MPa, and 17.5, 20, 25MPa, respectively. In order to understand the correlation between the formed hollow structure and the injected gas/water pressure, two parts with gas pressure of 10 and 20MPa were sectioned in the UT-B location. Figure 18 presents the photograph of these two sectioned parts. It is clearly seen that the part with gas pressure of 10MPa has a serious deformation and more bubbles existing in the inner surface of the hollow structure. But the part with gas pressure of 20MPa presents a uniform shape and fewer bubbles.

Here, the external diameter distribution, a parameter representing the level of deformation for the molded hollow structure, was presented with gas/water injection pressure. The external diameter distribution can be calculated by: $(D_{max}-D_{min})*100\%/D_{min}$, where D_{max} and D_{min} were the external maximum and minimum diameters in each UT location. A caliper, with accuracy of ±0.02mm, was used to measure the diameter. The measured diameter distributions in UT-A, B and C location, represented by square (■), circle (●) and triangle (▲), respectively, with respect to the gas pressure were presented in Figure 19. The diameter distributions in three UT locations were less than 1% when the gas pressure was 20MPa. However, those were from 4.6% to 9.9%, with respect to UT-A to UT-C location, respectively, when the gas pressure was 12MPa.

Ultrasonic contact duration may also present the relationship between the cooling efficiency and external diameter distribution. Figure 20 and 21 present the ultrasonic contact duration with respect to different liquid (gas or water) pressure in gas/water assisted injection moulding process. Ultrasonic contact duration increases with liquid pressure (gas or water), except part 31 (10MPa) and part 41 (20MPa) indicated by arrows in figure 20. When the liquid (gas or water) pressure was less than 20MPa, the contact duration was not stable and lower. The contact durations of WAIM are less than GAIM., indicating the cooling efficiency of water is higher than gas. These results showed that insufficient gas pressure would cause insufficient cooling for moulded part, part deform during cooling and/or part detachment, and the deformed level would increase with the distance from the gas/water nozzle. In addition, these data provide valuable insights into the actual processing conditions that can be utilized to validate the results from mould filling simulations.

6. Conclusions

A non-invasive ultrasound sensor system has been applied to the mould for both gas and water assisted injection moulding. The system has successfully detected both the arrival of polymer melt and the arrival of either the gas or water bubble that penetrates through the moulten polymer. A cavity mounted pressure transducer validated the introduction of gas or water into the cavity and changes in the ultrasound energy transmission into the melt along with echoes from the fluid polymer boundary were observed. The strength of reflected ultrasound energy from the fluid polymer interface is highest for the gas assisted case where the echo can clearly be detected. However, although the strength of reflection from the polymer water boundary is detectable it is weak and difficult for the automated signal processing system to pick out.

The utilisation of two ultrasound sensors allowed for the progression of the gas bubble through the polymer melt to be detected as the bubble arrival at each sensor location could be detected. The bubble arrival at each sensor also allowed for an estimation of the gas bubble velocity to be made at various gas injection pressure settings. As the gas pressure setting increased an expected increase in gas bubble tip velocity between sensor locations was observed.

The ultrasound energy reflected from the cavity boundary increases as the polymer detaches from the cavity wall since the acoustic coupling is impaired. This phenomenon allows for estimation for the length of time that the polymer remains in contact with the cavity wall. The cavity wall contact time was observed to be longer and more consistent with the higher fluid pressure settings. A higher post moulding deformation of the samples was observable where lower fluid pressure settings had been utilised.

The ultrasound data was used to estimate the residual wall thickness whilst the sample was in the mould. A reasonable correlation was made between the ultrasound estimate and the measured thickness using a Vernier thickness gauge after sectioning the sample components. Some scatter of the ultrasound thickness data was observed from the water assisted samples due to the inclusion of water voids within the residual wall.

Acknowledgements

EPSRC, Battenfeld UK and GmbH, A. Schulman Polymers, BP Chemicals, Kistler

References:

[1] J. Zhao, X. Lu, et. al., *SPE ANTEC Tech Papers*, **44,** 454-459 (1998).

[2] S. Y. Yang and S. J. Liou, *SPE ANTEC Tech Papers*, **40,** 404-407 (1994).

[3] T. Pearson, Gas assisted moulding for improved process economics, Materials World, 119-121, **3**(3), March, 1995.

[4] M. Knights, Plastics technology online article, http://www.ptonline.com/articles/200509fa1.html, (Sep. 2005)

[5] H. Eckardt, Polymer Process Engineering, 121-155, University of Bradford, UK, June 2001.

[6] L. Piché, A. Hamel, R. Gendron, M. Dumoulin, and J. Tatibouët, US Patent 5,433,112, 1995.

[7] C. L. Thomas, A. A. Tseng, J. L. Rose, and A. J. Bur, *SPE ANTEC Tech Papers*, **39,** 143 (1993).

[8] C. L. Thomas, A. O. Adebo, and A. J. Bur, *SPE ANTEC Tech Papers*, **40,** 2236 (1994).

[9] C. L. Thomas, M. Jiang, C. C. Chen, and A. J. Bur, *SPE ANTEC Tech Papers*, **41,** 2707 (1995).

[10] S.-S. L. Wen, C.-K. Jen, and K.T. Nguyen, *Int'l Polymer Processing*, **XIV**, 175-182, 1999.

[11] E.C. Brown, T.L.D. Collins, A.J. Dawson, P. Olley, and P.D. Coates, *J. Reinf. Plast. Comp.*, **18**, 331-338, 1999.

[12] Y. Ono, C.-C. Cheng, M. Kobayashi, and C.-K. Jen, *Polymer Engineering and Science*, **45**, 606-612, 2005.

[13] M. Kobayashi and C.-K. Jen, *Smart Materials and Structures*, **13**, 951-956, 2004.

[14] M. Kobayashi, Y. Ono, C.-K, Jen, and C.-C. Cheng, IEEE Sensors Journal, Vol. 6, pp. 55-62, 2006.

[15] A.R. Selfridge, IEEE transc. Sonics and Ultrasonics, **SU-32**, 3, 381-394, 1985.

[16] Cox, B. G., J. Fluid Mechanics, **14**, 81-96, 1962.

[17] F. Belblidia, J.F.T. Pittman, A. Polynkin, J. Sienz, Chemical Engineering Science, **60**, 4953 – 4956, 2005.

[18] Olley P, Mulvaney-Johnson L, Coates P.D.,. Plastics, Rubber and Composites, 47-58, **35**(2), 2006.

[19] H. Wang, B. Cao, C. K. Jen, K. T. Nguyen, and M. Viens, Polymer Engineering and Science, vol.37, no.2, pp.363-376, Feb. 1997.

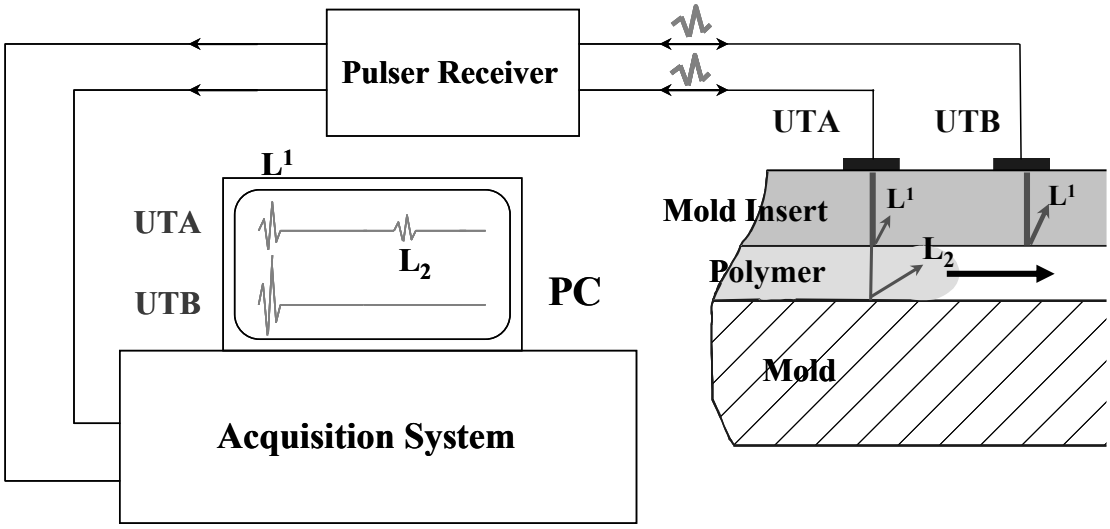

Figure 1: The cross-sectional schematic view of the mould with the UTs and data acquisition system for ultrasonic diagnostics of the injection moulding process using an ultrasonic pulse-echo technique.

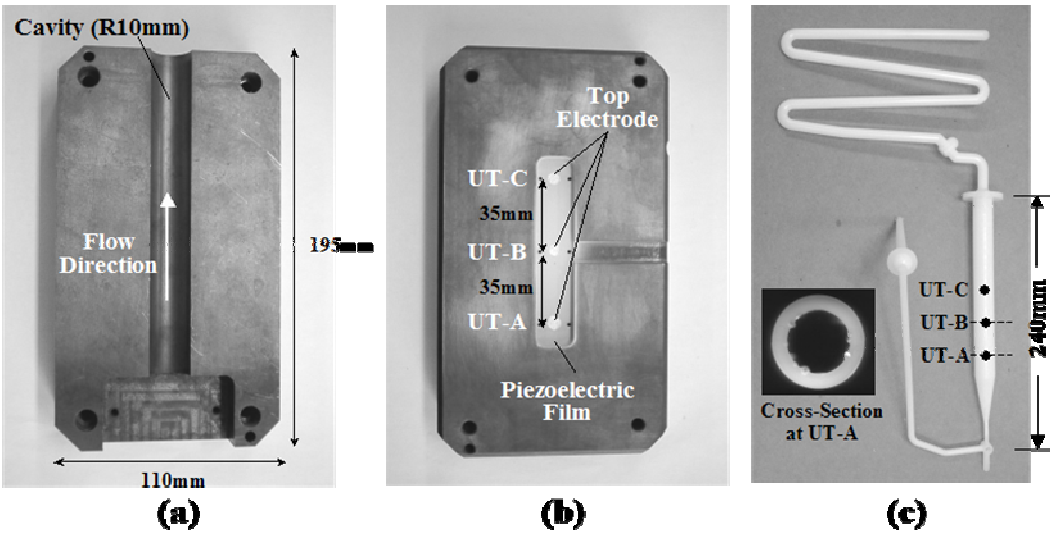

Figure 2: Photographs of (a) polymer side of mould insert having a half cylindrical cavity with a radius of 10mm, (b) three HTUTs (UT-A, B, C) fabricated on opposite side of the cavity, and (c) a moulded part, with gas/water assisted injection moulding.

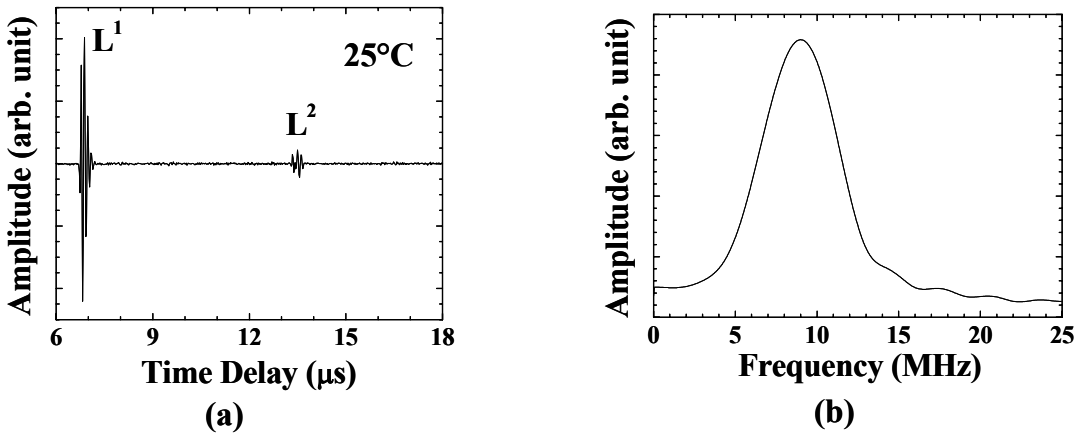

Figure 3: The performance of the ultrasonic sensor UT-A (a) in time and (b) in frequency domain at room temperature.

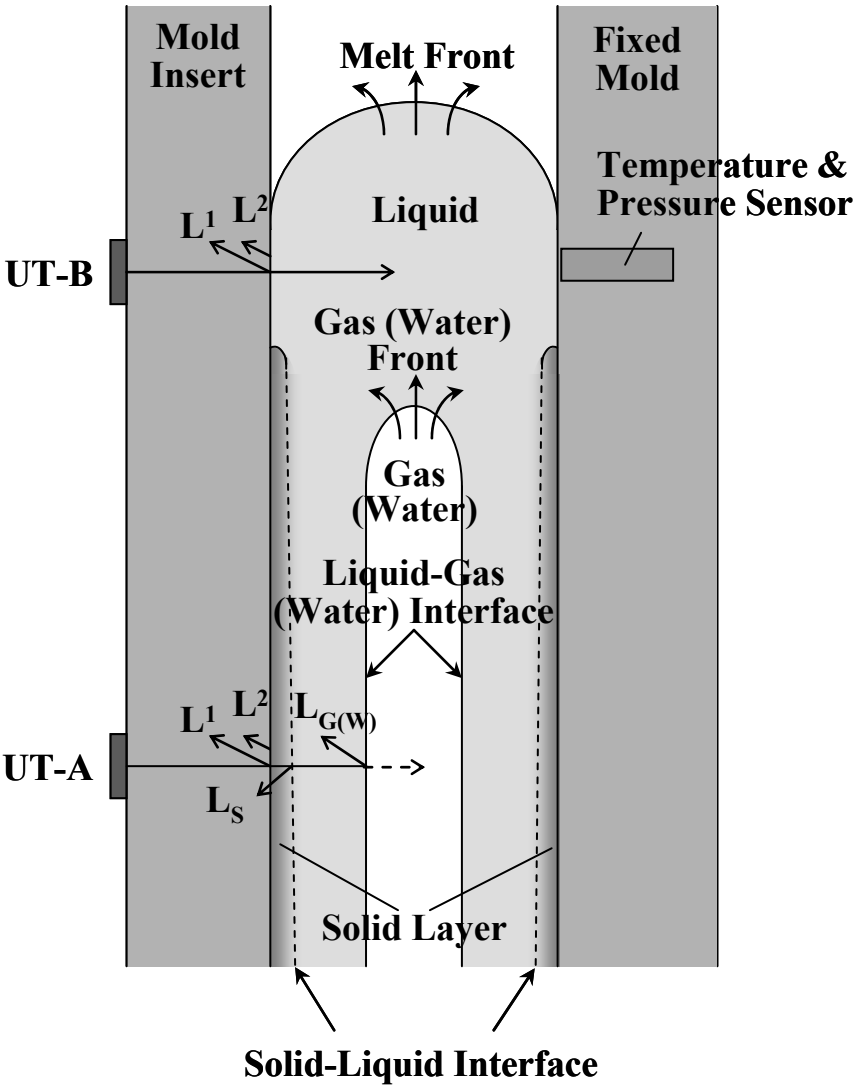

Figure 4: A schematic cross-section of the mould with UTs with ultrasonic propagation paths and flows of polymer melt and fluid (gas or water) in the cavity, with gas/water assisted injection moulding.

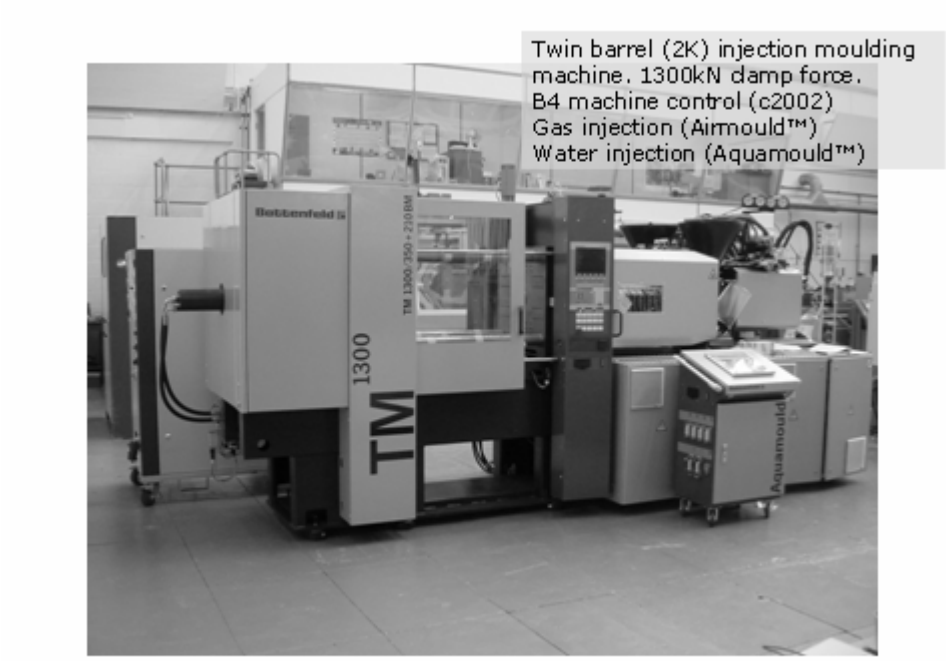

Figure 5: Battenfeld injection moulding machine with separate gas / water injection controller shown in the foreground. The water injection reservoir is shown behind the machine.

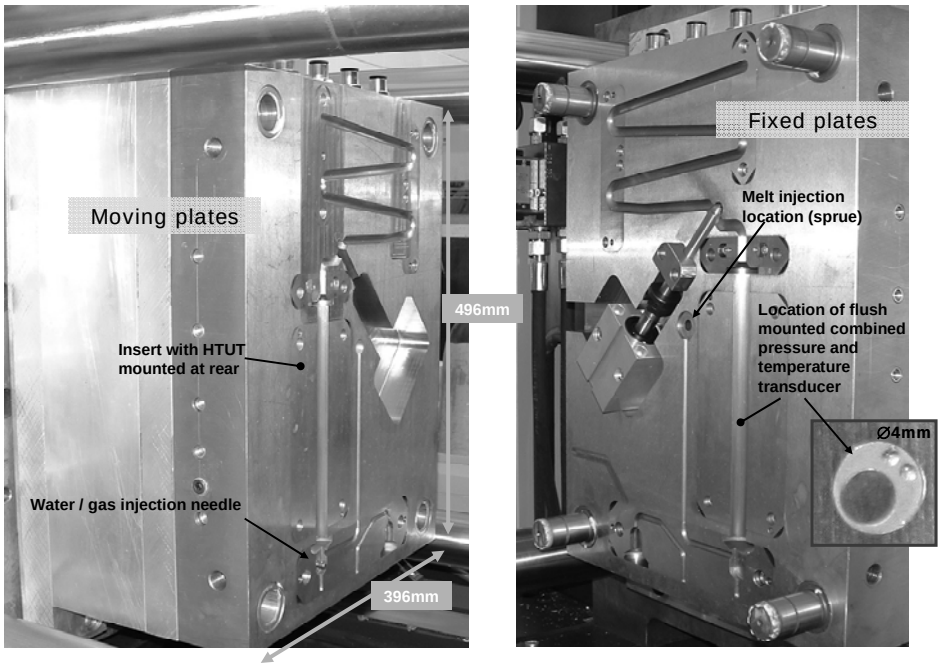

Figure 6: The combined water and gas assist moulding tool showing a cavity form that is made up from interchangeable inserts. The ∅20mm straight tube insert fitted with HTUT (moving side) along with combined peizo-electric pressure and thermocouple temperature transducer (fixed side) is shown.

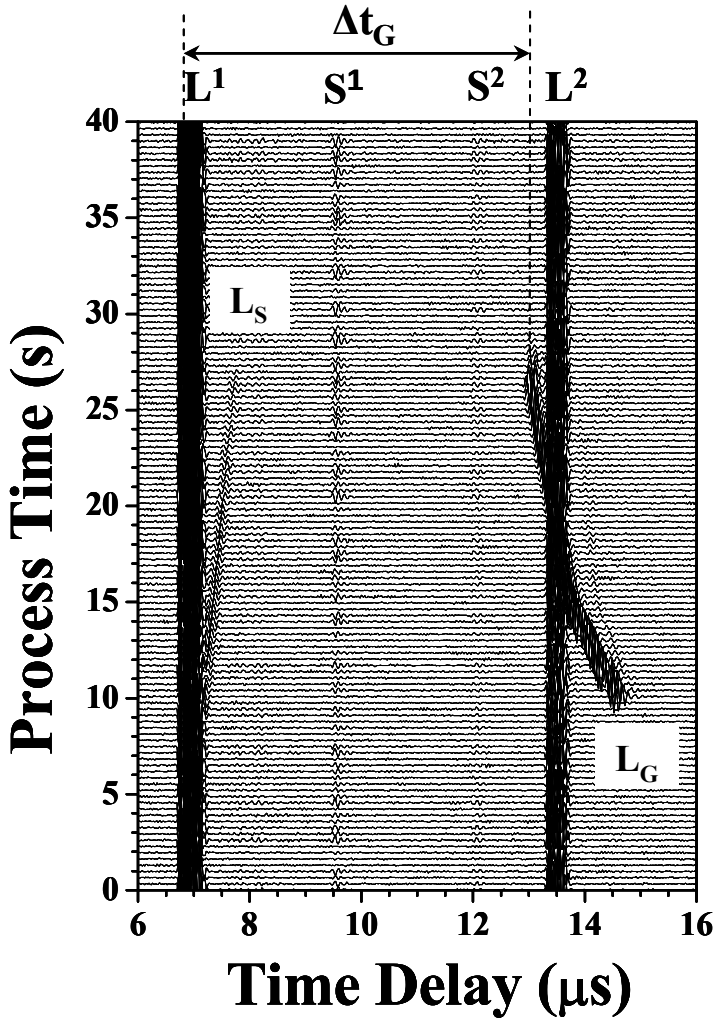

Figure 7: Typical signals acquired during one cycle of gas assisted injection moulding process.

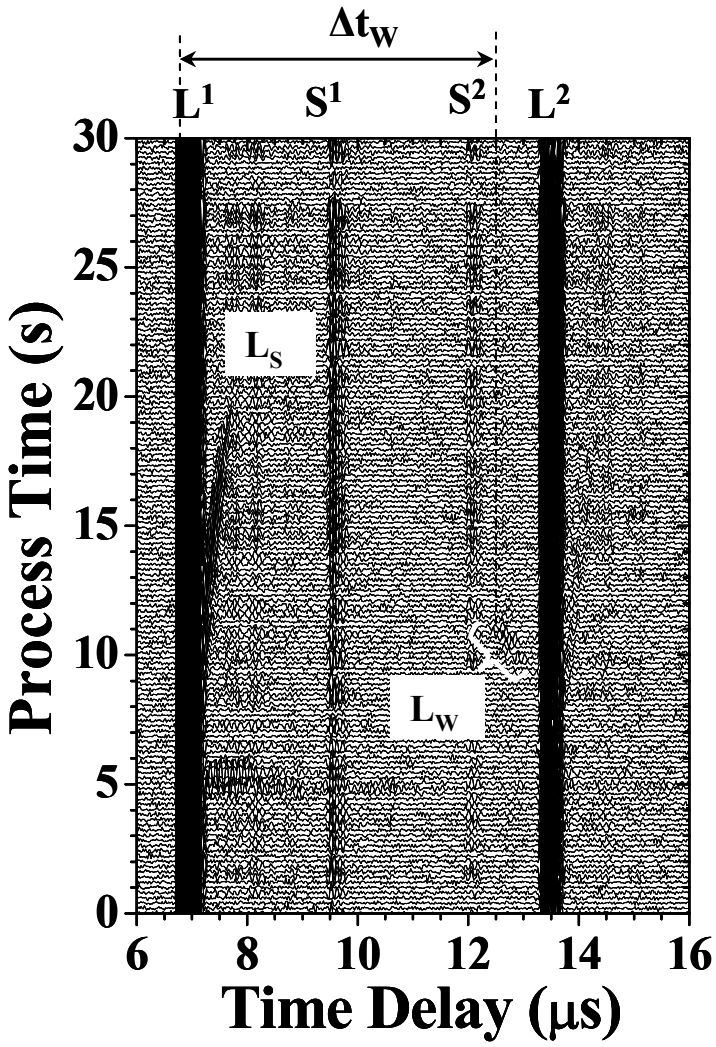

Figure 8: Typical signals acquired during one cycle of water assisted injection moulding process.

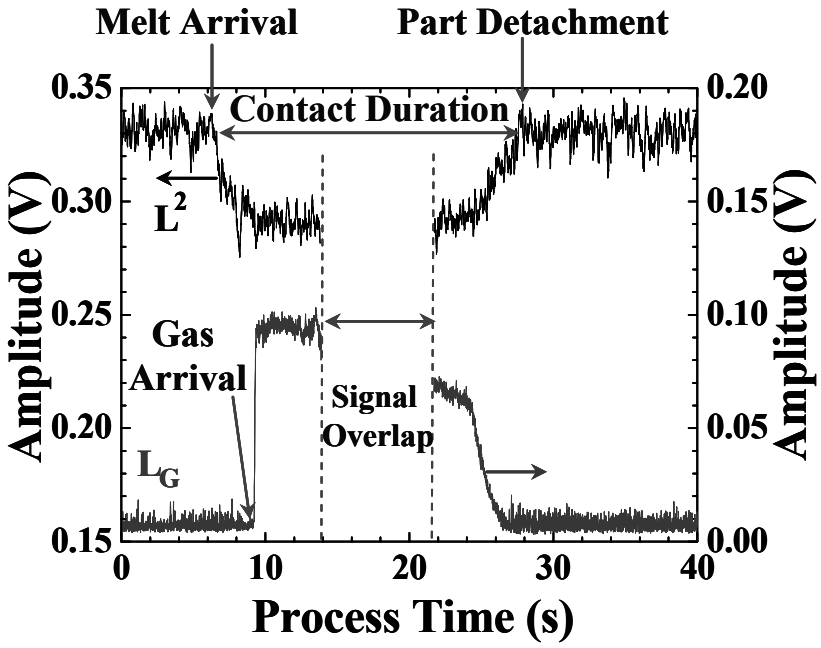

Figure 9: Amplitude variations of L^2 and L_G echoes, measured by UTA with respect to the process time.

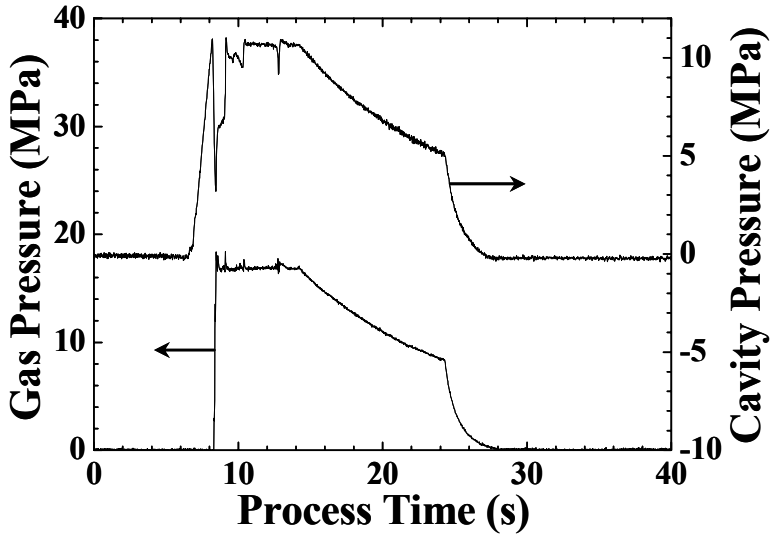

Figure 10: Amplitude variations of gas pressure, supplied by the gas machine, and cavity pressure, measured by the pressure sensor facing to the UTB, with respect to the process time.

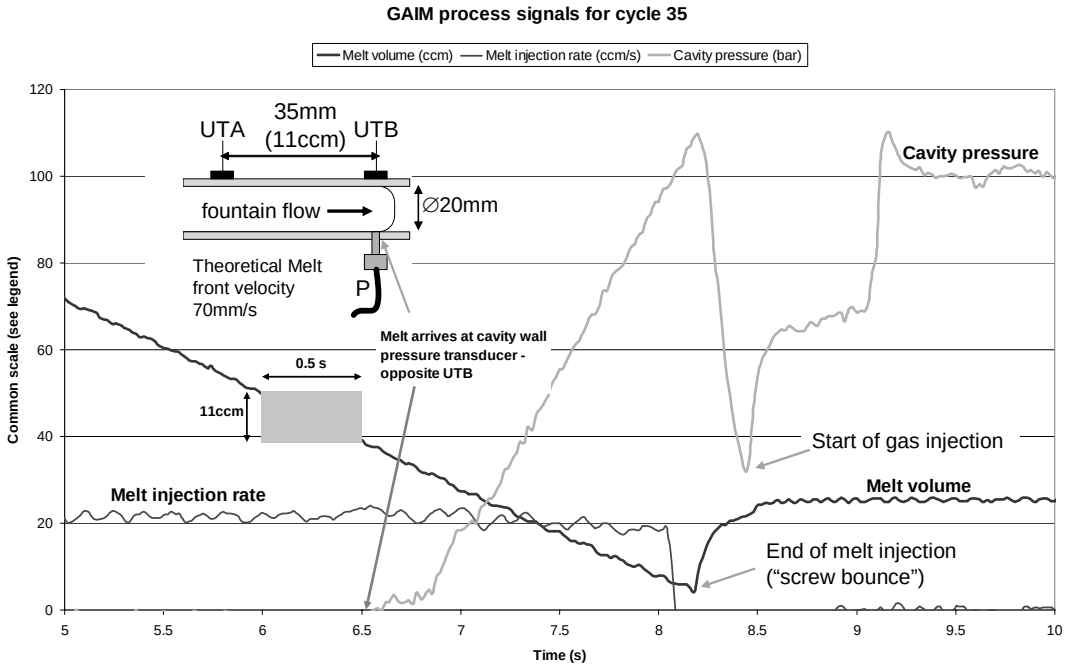

Figure 11: Process signals showing the displacement of the melt injection screw (falling melt volume in front of screw), the rate of melt delivery to the mould and the cavity wall pressure at the UTB location.

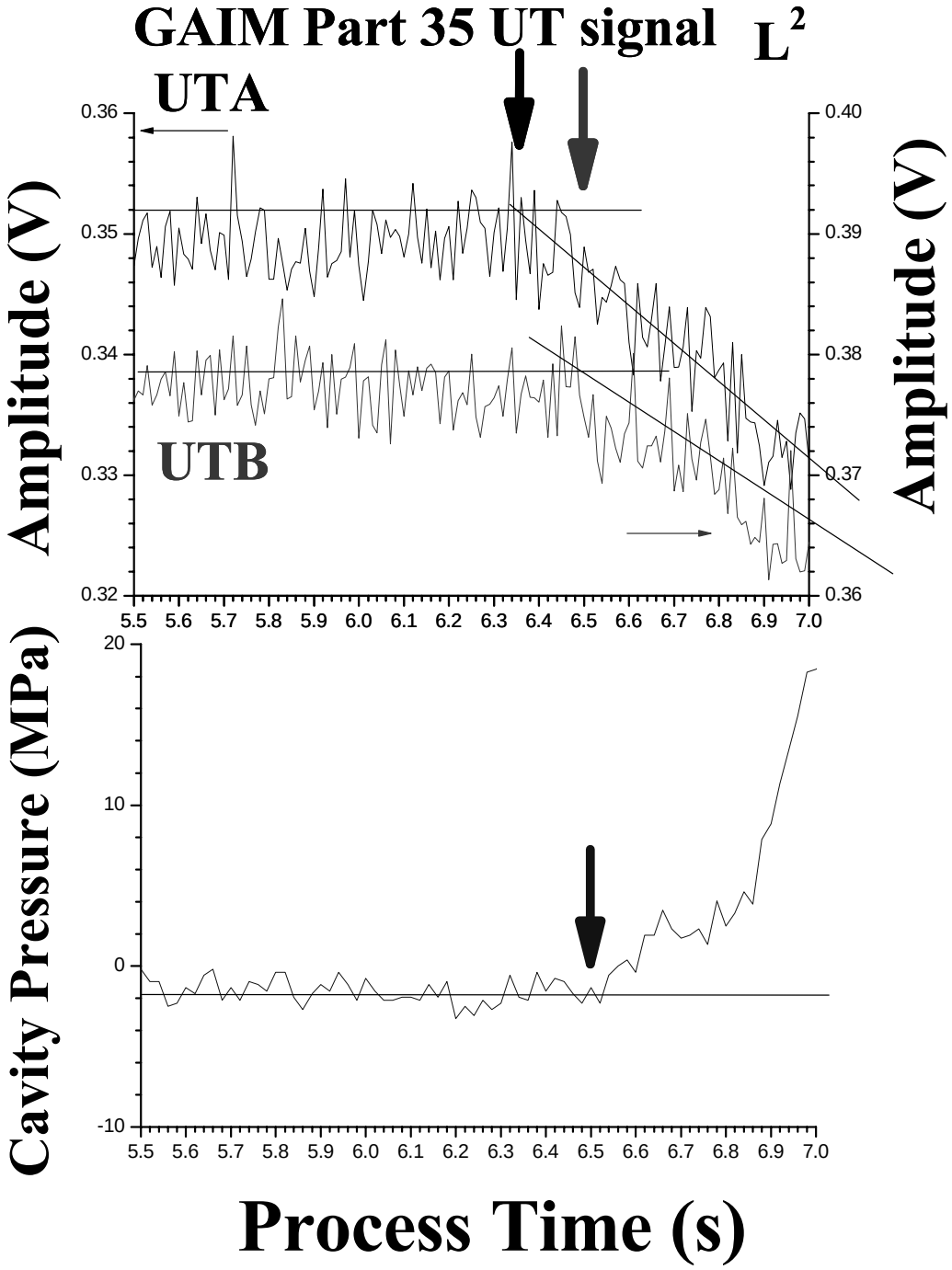

Figure 12: Melt arrival at the cavity wall is denoted by a fall in the UT signal amplitude. Here the signal amplitude for UTA and UTB is shown. The cavity pressure at the same location along the specimen as UTB increases as the melt passes over the transducer.

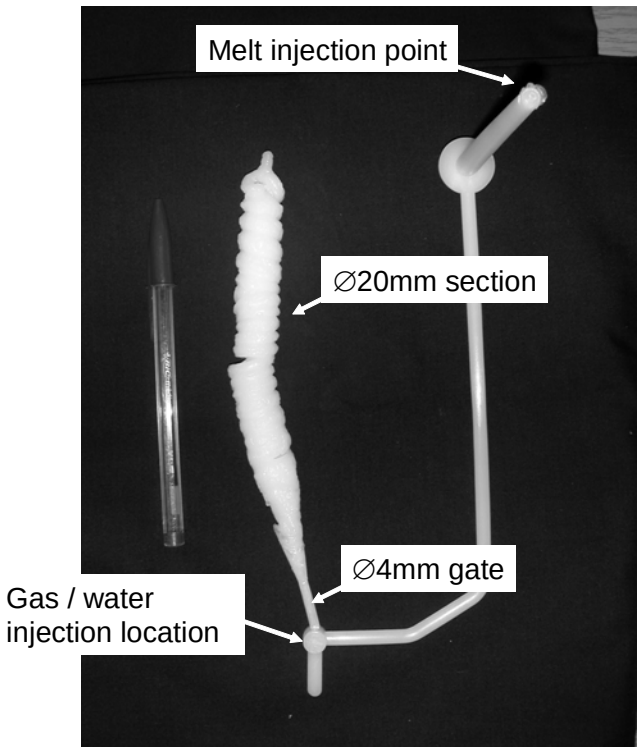

Figure 13: The form of melt at the end of melt pre-filling and prior to the injection of gas or water. The coiled form clearly indicates that "jetting" of the polymer melt from the ∅4mm gate has taken place within the ∅20mm section of the cavity.

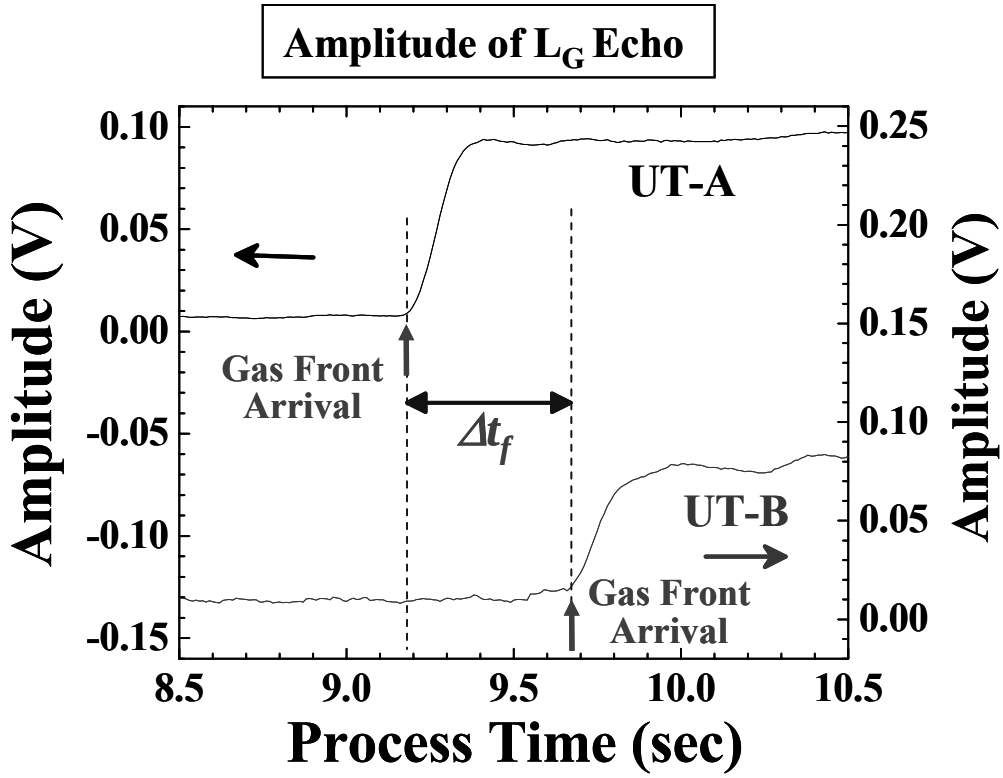

Figure 14: Amplitude variations of L_G echoes, measured by UT-A and UT-B, with respect to the process time. Rapid increase of the amplitudes indicates the gas front arrival at each UT location.

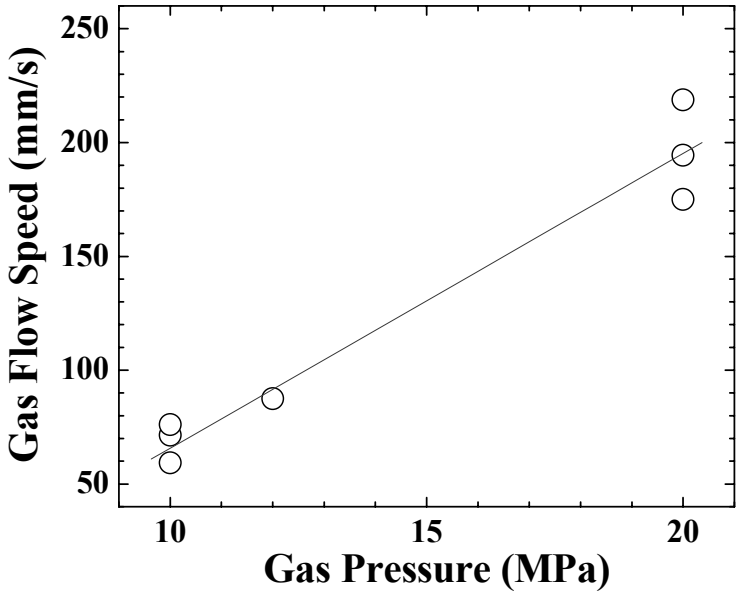

Figure 15: Gas flow speed between the UT-A and UT-B measured by ultrasonic technique with different gas pressures.

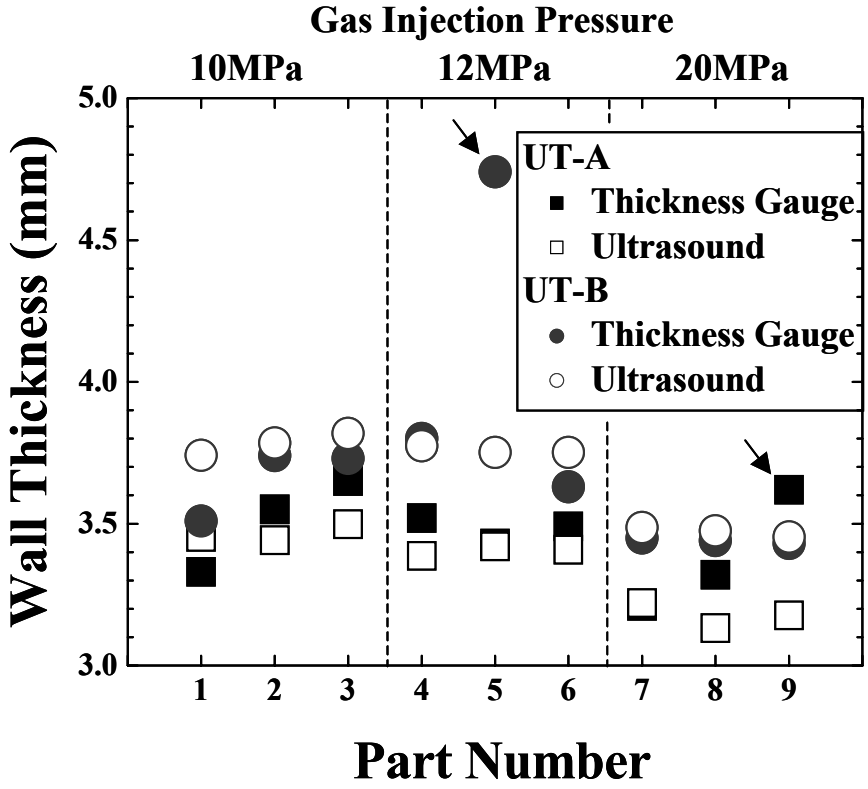

Figure 16: Comparison of wall thicknesses measured by thickness gauge after sectioning the parts and those estimated by ultrasonic technique during moulding with different gas pressures.

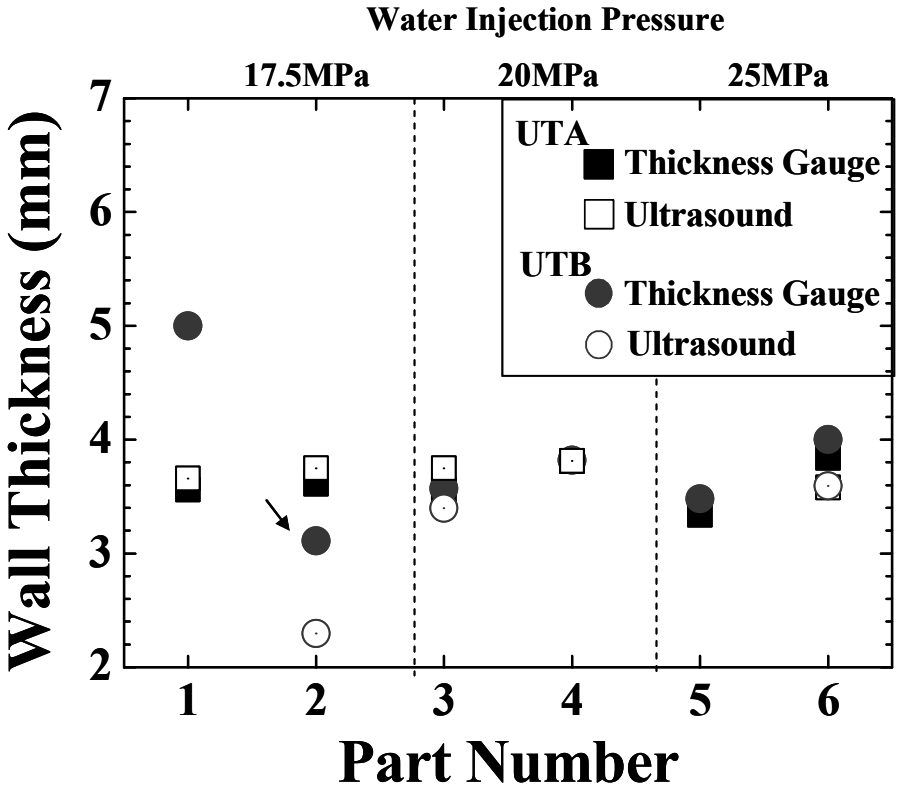

Figure 17: Comparison of wall thicknesses measured by thickness gauge after sectioning the parts and those estimated by ultrasonic technique during moulding with different water pressures.

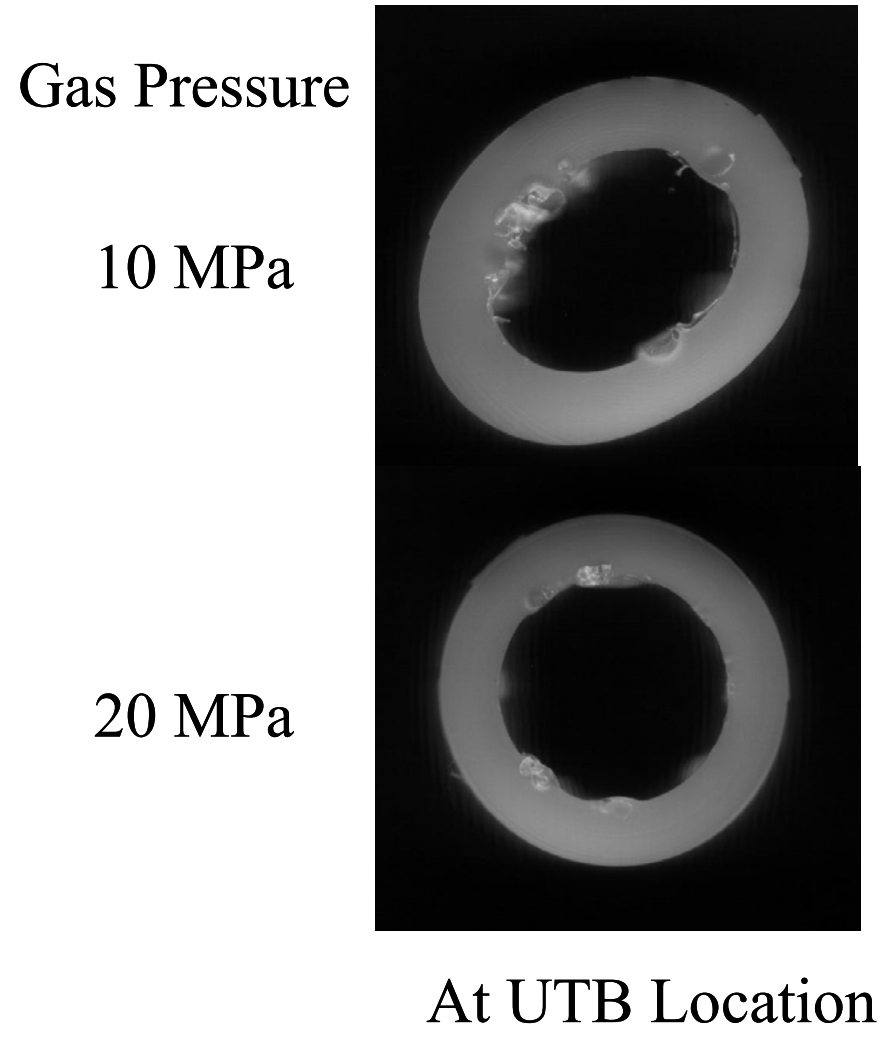

Figure 18: Photograph of the sectioned parts at the UTB location with respect to gas pressure of 10 and 20MPa.

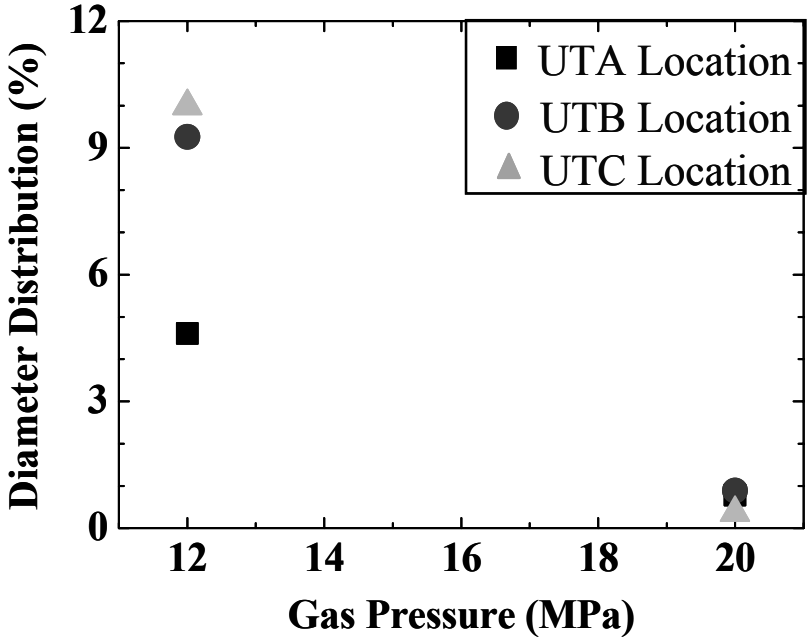

Figure 19: External diameter distribution of the moulded parts at UT-A, B, and C locations with respect to different gas pressures in gas assisted injection mould process.

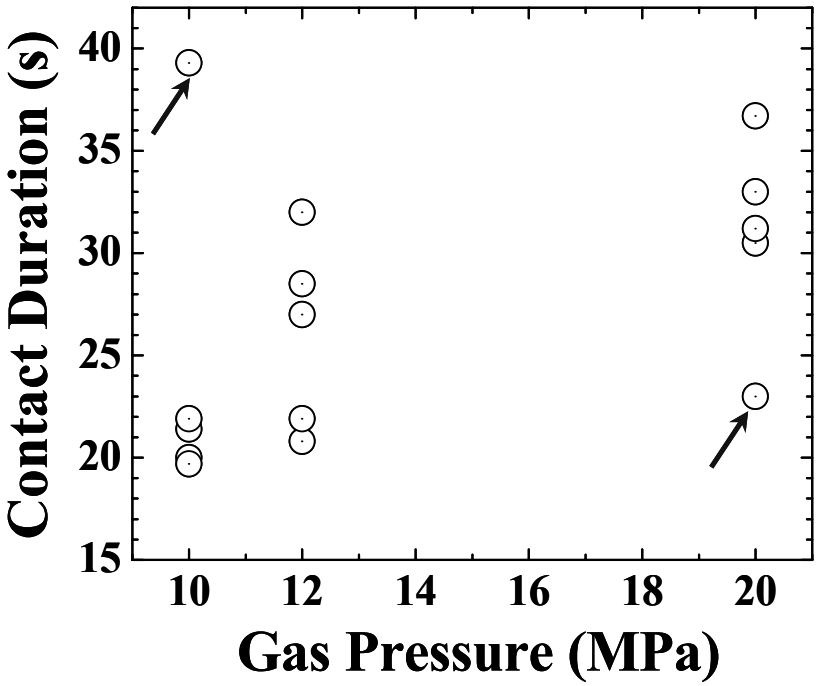

Figure 20: Ultrasonic contact time measured by UT-B, during the gas assisted injection molding process, with respect to different gas pressures.

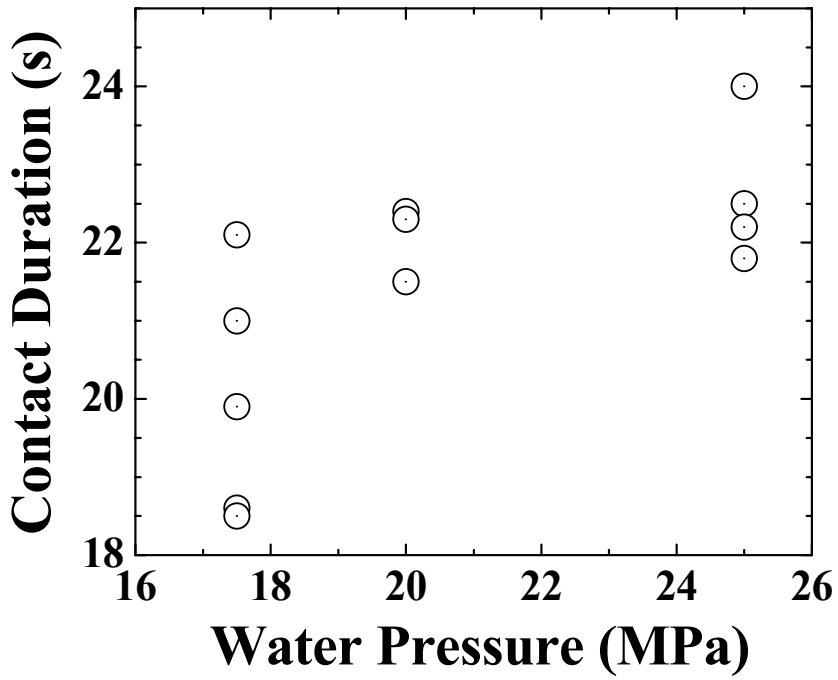

Figure 21: Ultrasonic contact time measured by UT-B, during the water assisted injection molding process, with respect to different water pressures.